Accumulation of worn-out GBM material substantially contributes to mesangial matrix expansion in diabetic nephropathy

Kriz, Wilhelm; Loewen, Jana; Federico, Giuseppina; van den Born, Jacob; Groene, Elisabeth; Groene, Hermann Josef

Published in:
American journal of physiology-Renal physiology

DOI:
10.1152/ajprenal.00020.2017

Am J Physiol Renal Physiol 312: F1101–F1111, 2017.
First published February 22, 2017; doi:10.1152/ajprenal.00020.2017.

RESEARCH ARTICLE | *Mechanism and Treatment of Renal Fibrosis*

Accumulation of worn-out GBM material substantially contributes to mesangial matrix expansion in diabetic nephropathy

Wilhelm Kriz,[1] Jana Löwen,[1,2] Giuseppina Federico,[2] Jacob van den Born,[3] Elisabeth Gröne,[2] and Hermann Josef Gröne[2]

[1]*Department of Neuroanatomy, Medical Faculty Mannheim, University Heidelberg, Germany;* [2]*Department of Cellular and Molecular Pathology, German Cancer Research Center, Heidelberg, Germany; and* [3]*Department of Internal Medicine, Division of Nephrology, University Medical Center Groningen, University of Groningen, The Netherlands*

Submitted 12 January 2017; accepted in final form 17 February 2017

Kriz W, Löwen J, Federico G, van den Born J, Gröne E, Gröne HJ. Accumulation of worn-out GBM material substantially contributes to mesangial matrix expansion in diabetic nephropathy. *Am J Physiol Renal Physiol* 312: F1101–F1111, 2017. First published February 22, 2017; doi:10.1152/ajprenal.00020.2017.—Thickening of the glomerular basement membrane (GBM) and expansion of the mesangial matrix are hallmarks of diabetic nephropathy (DN), generally considered to emerge from different sites of overproduction: GBM components from podocytes and mesangial matrix from mesangial cells. Reevaluation of 918 biopsies with DN revealed strong evidence that these mechanisms are connected to each other, wherein excess GBM components fail to undergo degradation and are deposited in the mesangium. These data do not exclude that mesangial cells also synthesize components that contribute to the accumulation of matrix in the mesangium. Light, electron microscopic, immunofluorescence, and in situ hybridization studies clearly show that the thickening of the GBM is due not only to overproduction of components of the mature GBM (α3 and α5 chains of collagen IV and agrin) by podocytes but also to resumed increased synthesis of the α1 chain of collagen IV and of perlecan by endothelial cells usually seen during embryonic development. We hypothesize that these abnormal production mechanisms are caused by different processes: overproduction of mature GBM-components by the diabetic milieu and regression of endothelial cells to an embryonic production mode by decreased availability of mediators from podocytes.

turnover of GBM components; production of mesangial matrix; resumption of embryonic GBM synthesis

DIABETIC NEPHROPATHY (DN) is a complex disease that may take years, even decades, to end up in end-stage renal failure. During this process, a great variety of structural changes are seen. The present study deals with mesangial matrix expansion, which is a hallmark of DN from its beginning. The original description by Kimmelstiel and Wilson in 1936 (25) of mesangial expansion as a nodular lesion (NS, nodular mesangial sclerosis) specific for diabetes was followed by the observation that a diffuse type of mesangial expansion (DMS, diffuse mesangial sclerosis) also occurs (8, 27). Since then, convincing evidence has been presented that both types of mesangial matrix expansion are almost invariably associated with each other, demonstrating that the nodular type emerges from the diffuse type (16, 20). These early studies already had revealed a further specific feature of DN, the prominent thickening of the glomerular basement membrane (GBM) (10, 11, 28).

The present study is part of a comprehensive reevaluation of biopsies of patients with type 1 and type 2 DN based on a total of 918 biopsies of both types. The present paper deals with the early stages of DN, including GBM thickening and mesangial matrix expansion, which shows that both phenomena are causally related to each other. In contrast to what is generally believed, mesangial matrix accumulation results, at least in a large part, from the accumulation of worn-out, undegraded GBM material in the mesangium.

MATERIALS AND METHODS

In total, 918 biopsies of DN from the years 2007–2015 (archive: Dept. of Cellular and Molecular Pathology, German Cancer Research Center, Heidelberg, Germany) were reevaluated. If not mentioned otherwise, biopsies without any histopathological changes were used as controls. The use of these materials was approved by the ethics committee of the University of Heidelberg Medical Faculty.

The biopsies consisted each of a tissue cylinder fixed in fresh 4% PBS-buffered formalin for 16–32 h at room temperature (25°C). After division, three to four pieces were embedded in paraffin (Paraplast), one piece (3 × 2 mm) was postfixed in OsO_4 and embedded in Araldite. The paraffin blocks were cut in 2- to 3-μm-thick sections that were routinely stained with PAS, Goldner-Trichrome a. o., and used for immunohistological assessments. The Araldite block was cut with a diamond knife to obtain 0.5-μm-thick sections that were stained with methylene blue and used for high-resolution light microscopy (LM) including the analysis of section series. Ultrathin sections were cut on an ultramicrotome, stained with uranyl acetate and lead citrate, and studied on Zeiss transmission electron microscopes (EM 9 or EM 901). Photographs were taken with an integrated digital Olympus MegaView G2 camera or a TRS-Tröndle CCD K2 camera.

Structural Analysis

In all biopsies a primary evaluation was done on PAS-stained paraffin sections. All glomeruli in a certain biopsy, generally displayed in several (~6–8) sections, were considered.

The degree of mesangial matrix expansion was taken to distinguish three groups: *1*) diffuse mesangial sclerosis (DMS), *2*) transitional stage from DMS to nodular sclerosis (NS), and *3*) NS (including "NS plus," comprising those with globular sclerosis). The assignment to one of these groups was done on the basis of which of the three pathologies was seen most frequently in the array of stained sections. Methylene blue-stained sections from plastic embedded material that

Address for reprint requests and other correspondence: W. Kriz, Dept. of Neuroanatomy, Medical Faculty Mannheim, University of Heidelberg. Ludolf-Krehl-Str. 13-17, Tridomus C, 68167 Mannheim, Germany (e-mail: wilhelm.kriz@urz.uni-heidelberg.de).

contained an assessable glomerulus were available from 804 biopsies. Selected samples were used for detailed analyses in serial sections and as pilot sections for transmission electron microscopy (TEM) studies.

Quantitative Assessments

The frequency analysis of the various pathologies was performed in PAS-stained paraffin sections. The assessment of the surface of gomerular capillaries was done in 0.5-μm plastic sections. The circumference of a capillary was divided into its fractions facing the GBM (filtering surface) and the mesangium, and both were separately measured using ImageJ 1.46r. All capillaries of a glomerular profile of seven biopsies each of early and late DMS were considered.

Immunofluorescence

Collagen IV chains. Paraffin sections were deparaffinized and incubated overnight with the antibodies listed below. The sections were treated before incubation with ProtK (Sigma) 20 mg/60 ml 15'/37°C. Since extensive control data were needed, unaffected portions of kidneys that had been surgically removed because of cancer served as controls.

Double incubations: collagen IV chains-synaptopodin. Immunofluorescence of collagens was done according to Wieslab Alport's Syndrome kit. After additional blocking of unspecific reactions with 10% fetal calf serum at room temperature for 10 min, the goat anti-synaptopodin antibody (listed below) was used 1:25 at room temperature for 60 min. The reaction was completed by the anti-goat AF 546-labeled secondary antibody listed below.

Double incubation: collagen IVα1-perlecan-agrin. Heat-induced epitope retrieval was performed using a DakoCytomation Pascal S2800 pressure chamber. Therefore, the deparaffinized renal sections were heated at 125°C for 7 min in 0.2 N HCl solution (pH 0.9).

After antigen retrieval, the sections were incubated with the first primary antibody, a rabbit anti-collagen IVα1 antibody (1:75 in 1% BSA-PBS, 25°C, 60 min). Sections were rinsed using PBS, and the first secondary antibody, a donkey anti-rabbit AF 488 antibody (listed below) was subsequently used to identify binding of the primary antibody.

After extensive washes in PBS, the second primary antibody, for perlecan a rat anti-perlecan antibody (1:100); for agrin a mouse anti-agrin antibody (1:500) was applied and detected by the second secondary antibody, for perlecan a rabbit anti-rat horseradish peroxidase (HRP); for agrin a goat anti-mouse HRP (listed below), followed by tyramide-TRITC staining.

Antibodies

Collagen IV-synaptopodin studies. For the Collagen type IV studies, the Collagen type IV: The Eurodiagnostika Wieslab Alport's Sydrome Kit ALP105RVO was used containing the following antibodies: collagen IVα1 MAB1 (1:25) mouse; collagen IVα3 MAB3 (1:100) mouse; collagen IVα5 MAB5 (1:50) rat; CD31: DAKO, CD31, monoclonal mouse (1:10); synaptopodin: Santa Cruz, synaptopodin (sc21537), goat (1:25); Secondary Fluorescence AK, Invitrogen: AF488 anti-rabbit (1:300); AF488 anti-mouse (1:400); AF488 anti-rat (1:300); AF 546 anti goat (1:300); cell nuclei: DRAQ5 (1:5).

Collagen IVα1 chain-perlecan-agrin studies. For the Collagen type IVα1 studies, the antibodies used were the following: Abcam, (ab189408) rabbit polyclonal (1:75); antibodies against the core protein of the basement membrane HSPGs: perlecan: Upstate Biotechnology, (A7L6) rat monoclonal (1:100); agrin: Van den Born, J. (JM72) mouse monoclonal (1:500); Secondary Fluorescence AK: Invitrogen AF488 anti-rabbit (1:250), Dako Diagnostics anti-rat Ig HRP (1:100), Southern Biotech anti-mouse IgG1 HRP (1:100), followed by tyramide-TRITC (1:50), PerkinElmer.

The samples were studied with a conventional fluorescence microscope and a confocal laser-scanning microscope Leica DMRBE or DMRE.

RNA In Situ Hybridization

Paraffin sections (5 ± 1 μm) were baked in a dry oven at 60°C for 1 h before the RNAscope assay application. Probes for collagen IVα1 and -α3 were developed by ACD (Advanced Cell Diagnostic, Hayward, CA). Staining was obtained using the RNAscope 2.5 HD Detection reagent (Advanced Cell Diagnostic).

The number of collagen-positive dots was counted in each glomerulus, and the average glomerular number per biopsy was calculated.

In Situ Hybridization Combined With Immunoflorescence

With the use of the RNAscope reagent kit with "Red" (no. 322350) as substrate, collagen IVα1 mRNA was shown (ACD). Consecutively, a mouse monoclonal anti-CD31 (1:10, DAKO) was applied overnight at 4°C. CD31 was displayed by the tyramide signal amplification method (TSA kit, streptavidin coupled to AF 488 (Invitrogen/Molecular Probes/Thermo Fisher Scientific, Schwerte, Germany).

RESULTS

Incidences

From all 918 biopsies we had PAS-stained paraffin sections. Diagnosis of all biopsies was done after performance of light microscopy, immunhistology for IgA, IgG, IgM, C1q, C3, and fibrinogen-fibrin and transmission electron microscopy (TEM). From 804 biopsies we had 1-μm plastic sections that contained a glomerulus and were allowed to evaluate the changes by high-resolution LM. We studied eight biopsies by IF, six biopsies by ISH, and two cases by combined IF/ISH (in situ hybridization).

In all biopsies, mesangial expansion was found as the most common feature of DN (Fig. 1). DMS (as the exclusive pathology) was encountered in 14%, the transitional stage from DMS to NS was seen in 34% as the dominant lesion and NS (including NS plus, i.e., with many glomerular profiles displaying global sclerosis) in 52%. Assessment of the frequency of GBM thickening was not possible in paraffin sections but was consistently found by TEM in all routine reports for all samples.

Histopathology

GBM thickening. Thickening of the GBM is the earliest structural change in DN, clearly preceding mesangial matrix expansion, as was first shown by Osterby et al. in 1974 (37). The thickened GBM caused a narrowing of the spaces within the GBM infoldings (compare Fig. 2*A* with Fig. 2*B* and Fig. 6*E* with Fig. 6*F*) that seemed to compromise the podocyte portions at this site (see next section). Outside these clefts, podocytes frequently exhibited an intact foot process pattern.

Diffuse mesangial sclerosis. Diffuse mesangial sclerosis (DMS) consisted of the accumulation of matrix within the mesangium accompanied by the narrowing and shortening of GBM infoldings. Podocytes progressively retracted out of the constricted spaces within the GBM infoldings accompanied by the shedding of cytoplasmic material into these spaces. This process left the innermost portions, i.e., the bends of the GBM infoldings, without podocyte support. These portions disconnected from the GBM and became included into the mesangium (Fig. 3, Fig. 4, and Fig. 5). Thereby, the mesangium expanded and its matrix prominently increased. Structural evidence for this process emerged from sequestered podocyte remnants that had become enclosed in the engulfed GBM

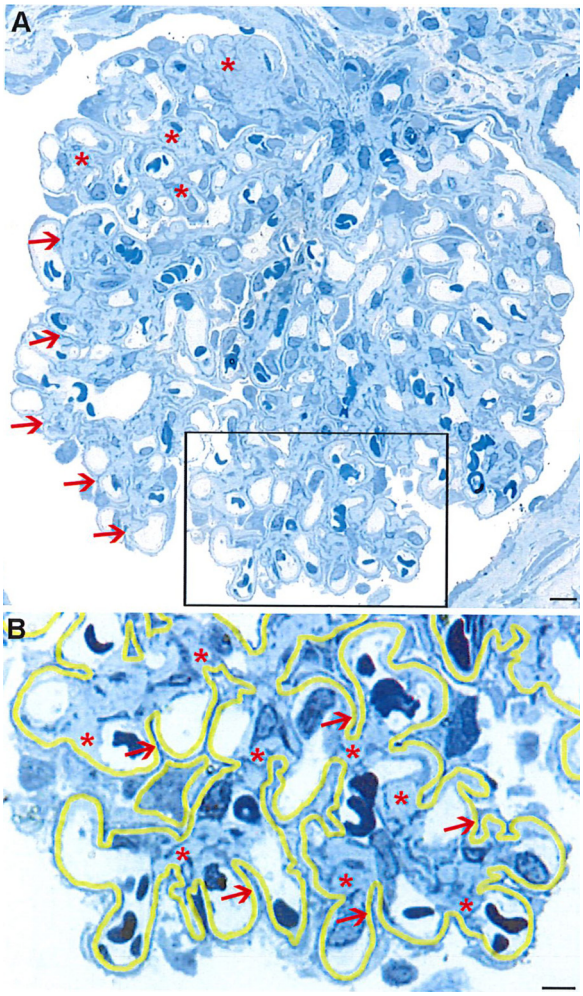

Fig. 1. Diffuse mesangial sclerosis (DMS). *A*: overview of an entire tuft showing the homogeneity of the changes in DMS, distinct in the zoom. Throughout the tuft, a thickened GBM and expansion of the mesangial matrix are seen. The accumulated matrix is generally associated with the bends of the GBM infoldings (asterisks), suggesting a dropping of the innermost GBM portions into the mesangium. Note the narrowness and shortening of the clefts within the GBM infoldings (arrows). *B*: highlighting of the GBM in the zoom clearly shows its homogenous thickening. diabetic nephropathy (DN) biopsy. Thin-section light microscopy (LM) stained with methylene blue. Scale bars, 20 μm.

matrix. These inclusions provided a label showing that this material was derived from the GBM.

Transitional stages from DMS to NS. The transitional stages from DMS to NS (Fig. 5*A*) were characterized by the increasing accumulation of matrix within the mesangium and by the progressive loss of the folding pattern of the GBM followed by a displacement of capillaries into the mesangium. As seen from our assessments, the filtering surface of capillaries decreased from 54.9% in early DMS to 28.9% in late DMS. Many capillaries lost any contact with the GBM, collapsed and finally degenerated. In contrast, capillaries on the outer surface of such lobules were well preserved and were covered with podocytes that frequently exhibited an intact pattern of interdigitating foot processes (Fig. 5). Evidence for detachments and loss of podocytes was not found.

Nodular sclerosis. The continuous deposition of GBM material derived from GBM infoldings appeared as the main factor for the progressive increase in mesangial matrix. This led to the impression of a progressive bulging of the GBM but was actually due to the cutting of infoldings (Fig. 5).

Nodular sclerosis (NS) developed through the confluence of the accumulated matrix associated with the disappearance of capillaries from central mesangial areas (Fig. 5*A*). At many sites, the nature of the matrix as undegraded GBM material was obvious by the enclosed matrix vesicles derived from podocytes (Fig. 5).

The early stage of NS (Fig. 5*B*) consisted of a central core of homogenous matrix (enclosed remnants of podocyte material

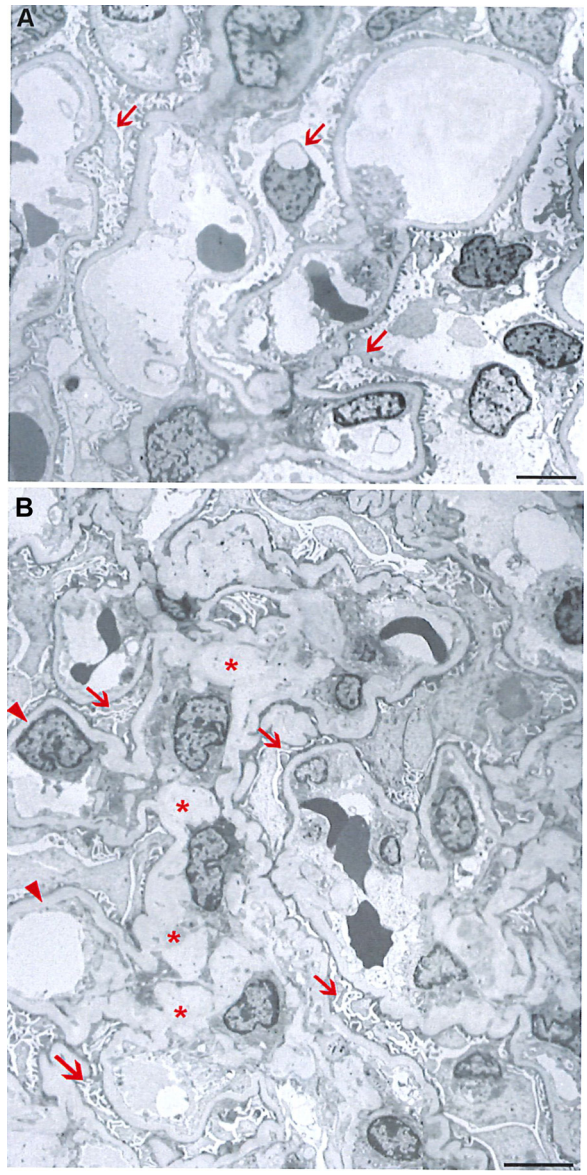

Fig. 2. Diffuse mesangial sclerosis. Compared with controls (*A*), the most conspicuous glomerular changes in DMS (*B*) consist of the accumulation of matrix within the mesangium and decreased width of the spaces within the GBM infoldings (arrows). At many sites, the deposited matrix in the mesangium is in continuity with the thickened innermost portions of the GBM infoldings (asterisks). Podocytes within the narrow GBM infoldings compared with *A* seem to be compressed and frequently show foot process effacement. Biopsies of a patient without any renal pathological changes (*A*) and of a patient with DN (*B*) are shown. Transmission electronmicroscopy (TEM). Scale bars, 5 μm.

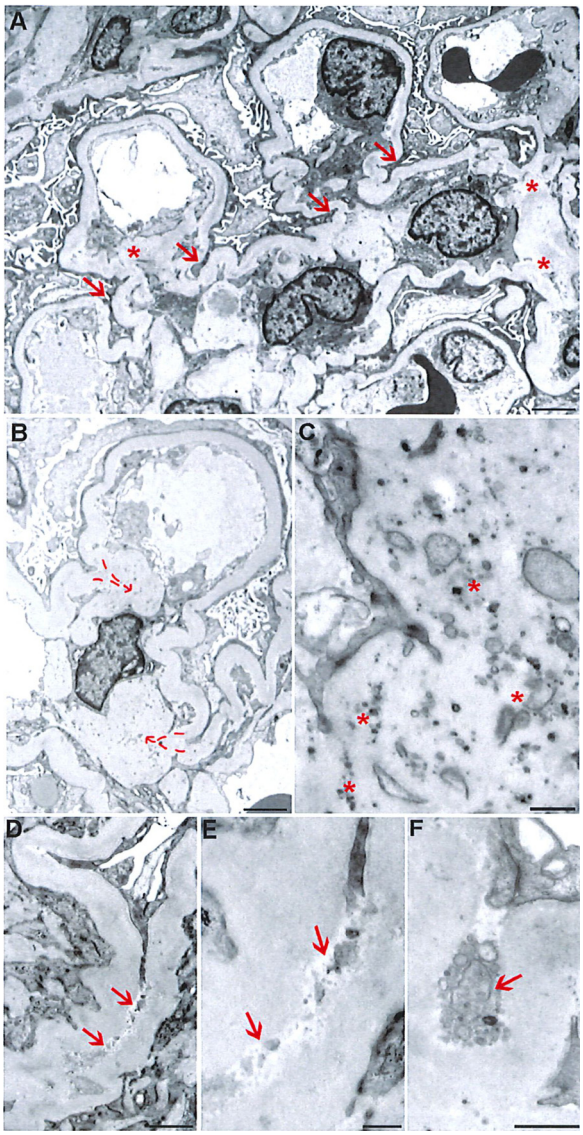

Fig. 3. DMS: incorporation of GBM portions into the mesangium. *A*: overview. Podocytes are in the process of retracting out of the narrow clefts within the GBM infoldings (arrows); asterisks label GBM material incorporated into the mesangium. *B*: single capillary and adjacent mesangium. The innermost portions of the GBM of both corresponding infoldings (curved arrows) have become part of the mesangium, as may be seen by the inclusion of podocyte-derived cytoplasmic material. *C*: high-power view of GBM material within the mesangium, which contains abundant podocyte matrix vesicles derived from shedding (asterisks). *D, E*, and *F*: high-power views of GBM infoldings showing the shedded cytoplasmic material of podocytes that is left behind in the bends of the GBM infoldings (arrows); *E* is a zoom of *D*. *A–F*, DN biopsy material, TEMs. Scale bars: *A* and *B*, 2.5 μm; *C*, *E*, and *F*, 0.5 μm; *D*, 1 μm.

were still seen) without capillaries but peripherally located mesangial cells, which varied in number between scarce and abundant. This central core was surrounded by a ring of capillaries covered, at their outer aspect, by the GBM and normal-looking podocytes. This stage appeared to be transient, since nodules with deranged surface capillaries and serious podocyte lesions, including detachments of podocytes, were much more frequently encountered (not shown).

Immunofluoresence data. The mature GBM contains the α3, α4, and α5 chains in addition, to a lesser degree, the α1 and α2 chains of collagen IV (1). The dominant proteoglycan of the mature GBM is agrin replacing the perlecan that is the major proteoglycan during development (18, 19).

By IF, we studied the distribution of the α1, α3, and α5 chains of collagen IV as well as agrin and perlecan.

As expected, the α3 and α5 chains were detected as major components of the GBM in biopsies of patients with DN and of controls. Whereas in controls minimal amounts of these chains were seen within the mesangium, at best, in DMS, accumulations of these chains were detected as an essential part of the expanded mesangial matrix. Since the results with the α3 and α5 chains were virtually identical, we show the results with only the α5 chain (Fig. 6). The staining of the deposits in the mesangium was in continuity with the staining of the GBM. In double incubations with synaptopodin, the occurrence of these chains within the GBM and the additional accumulation in the mesangium were also clearly seen. Central regions of the mesangium including the matrix in nodules were mostly not stained.

The staining pattern of the α1 chain of collagen IV clearly differed from that of α3 and α5 chains. In controls, weak staining for the α1 chain was encountered in the GBM in an irregular pattern, frequently together with sporadic accumulations in the mesangium (Fig. 7*A*). In DN, the α1 chain of collagen IV was always brightly seen in high density within the expanded mesangial matrix, maintained also in nodules. Surprisingly, the GBM itself was also frequently stained, regionally intensively, even in cases in which the corresponding mesangium was unstained (Fig. 7, *B–F*).

The IF-staining for agrin largely corresponded to the staining pattern of the α3 and α5 chains of collagen IV in controls and DN (not shown). In contrast, the staining pattern for perlecan was similar to that of the α1 chain of collagen IV, weak in controls (Fig. 7*G*); in DN the GBM presented as thin line, the mesangial matrix was brightly stained (Fig. 7*H*).

In situ hybridization. In situ hybridization with probes for α1 and α3 chains of collagen IV confirmed that the α3 chain is synthesized by podocytes (Fig. 8, *A* and *B*), the α1 chain by cells inside the GBM, most likely by endothelial cells, but a clear separation from mesangial cells was not possible (Fig. 8, *C* and *D*). Therefore, in a separate approach, we combined ISH for the α1 chain of collagen IV, with the IF staining of the endothelial marker CD31 (Fig. 8*E*) verifying that the α1 chain is synthesized by endothelial cells, not by podocytes or mesangial cells.

In the first experiment in a semiquantitative assessment in comparison with controls, we counted the ISH-positive dots for the α1 and α3 chains per glomerulus and calculated the average number of ISH-positive dots per biopsy. We found that with respect to the α3 chain there was no change in RNA transcripts compared with controls; with respect to the α1 chain there was an increase in some biopsies of DN. However, on average, a significant difference was not found (Fig. 8*F*).

DISCUSSION

The present study provides strong evidence that the specific matrix accumulation in the mesangium in DN is due, at least in substantial part, to a dropping of GBM material into the mesangium. This is in contrast to what is generally believed, namely that the masses of mesangial matrix in DN are directly

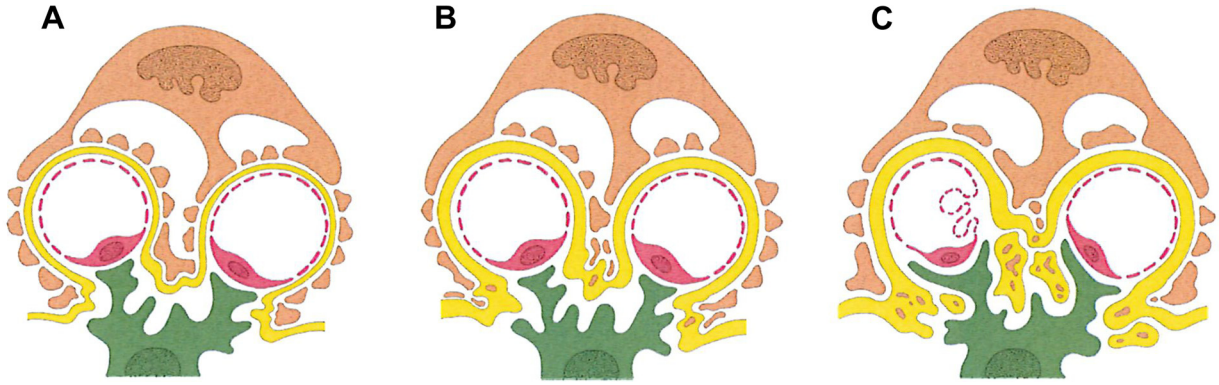

Fig. 4. Schematics showing sequence of GBM engulfment. The GBM is shown in yellow, the podocyte in pink, the mesangial cell in green, and capillaries in red. *A* normal *B* thickening of GBM, retraction of podocytes out of the constricted GBM infoldings, leaving behind shed cytoplasmic material. *C*: dropping of the innermost portions of the GBM into the mesangium; these portions contain shed cytoplasmic material from podocytes. Capillaries lose contact with the GBM and start to collapse.

and only produced within the mesangium by mesangial cells. This raises the question where and by which cell type under normal conditions the various components of the GBM are produced and where and by which they are degraded.

First of all, the turnover of the GBM is slow. Classic metabolic labeling studies done 40 years ago showed that the in-vivo loss of GBM protein radioactivity has a half-life of more than 100 days (39). Walker before, in 1973, using a silver impregnation labeling technique, reached a similar value (45). Thus, GBM components are extremely long lived. No detailed studies are available about individual components.

The α3, α4, and α5 chains of collagen IV are specific for the mature GBM synthesized by podocytes (1). The α1 and α2 chains of collagen IV are typically found during glomerular development but are encountered in small amounts also in the mature GBM produced by endothelial cells (3, 22). Agrin is the specific proteoglycan of the mature GBM produced by podocytes, whereas perlecan is normally found only during glomerular development up to the capillary loop stage and considered to be synthesized by endothelial cells (18, 19).

The GBM exhibits a stratified arrangement of its components with laminins and agrin at the endothelial and epithelial sites, whereas the collagen IV chains occupy the central region, with the α1 and α2 chains of collagen IV found only within the inner central region (41), consistent with their surmised synthesis by endothelial cells.

Little is known about the site of GBM degradation. Walker (45) concluded from the movements of the silver labels over time that the newly produced components move from a peripheral position within the GBM slowly to more central layers and, when the labeled components have reached the lamina rara interna, they are carried laterally toward a perimesangial position, being finally incorporated into the mesangial matrix and degraded by mesangial cells in some way or another. This process took about a year to be completed. A major problem with these results consists of not knowing which components of the GBM had been labeled by this impregnation technique. However, these experiments allow the conclusion at least that components of GBM are degraded in the mesangium. The idea that worn-out GBM is degraded in the mesangium has been raised in early studies also by others (2, 14, 35) but has never been seriously explored.

The degradation of GBM material depends on metalloproteinases (MMPs). These are secreted or, to a lesser degree, membrane-bound enzymes which are subject to regulation by specific inhibitors and stimulators (29). The question how matrix degradation (GBM and mesangium) proceeds in DN has been addressed in many studies. It was found that the overall turnover of matrix proteins in DN is compromised by decreased MMP expression, decreased levels of MMP activators, and increased expression of MMP-inhibitors (12, 29, 30, 47). Moreover, the metabolic situation with increased formation of advanced glycation end products of collagen IV and laminins markedly decreases their susceptibility to cleavage by MMPs (12, 29, 30).

There are many reports that the accumulated matrix in the mesangium in DN has a basement membrane-like appearance, frequently termed basement membrane-like material (5, 21, 23, 33, 35, 38, 45). However, the increase of matrix in the GBM and in the mesangium were considered to evolve in parallel but from different production sites, from podocytes and mesangial cells, respectively. The hypothesis that the accumulated matrix in the mesangium derives from an accumulation of worn-out undegraded GBM material has never been seriously considered.

We clearly show that, at the least, a substantial portion of the accumulated matrix in the mesangium in DN is derived from the deposition of GBM material. The evidence based simply on the inspection of high-resolution LMs and, most reliable, on TEMs is conclusive. The mechanism consists of the retraction of podocytes out of the spaces between the GBM infoldings followed by the incorporation of the podocyte-deprived bends of the GBM infoldings into the mesangium. Such a process has never been described for any other glomerular disease but may occur in the same manner in other glomerular diseases, e.g., glomerular changes in nephrosclerosis (32). The retraction of podocytes seems to be the consequence of the constriction of the spaces within the GBM infoldings (suggestively due to the thickening of the GBM), not of a prior regulatory defect of podocytes. The fact that during this process podocytes sequester cytoplasmic portions into the clefts just mirrors the general propensity of podocytes to sequester cytoplasmic portions (26). Along with the retraction out of the clefts of the GBM infoldings, podocytes regularly dropped off

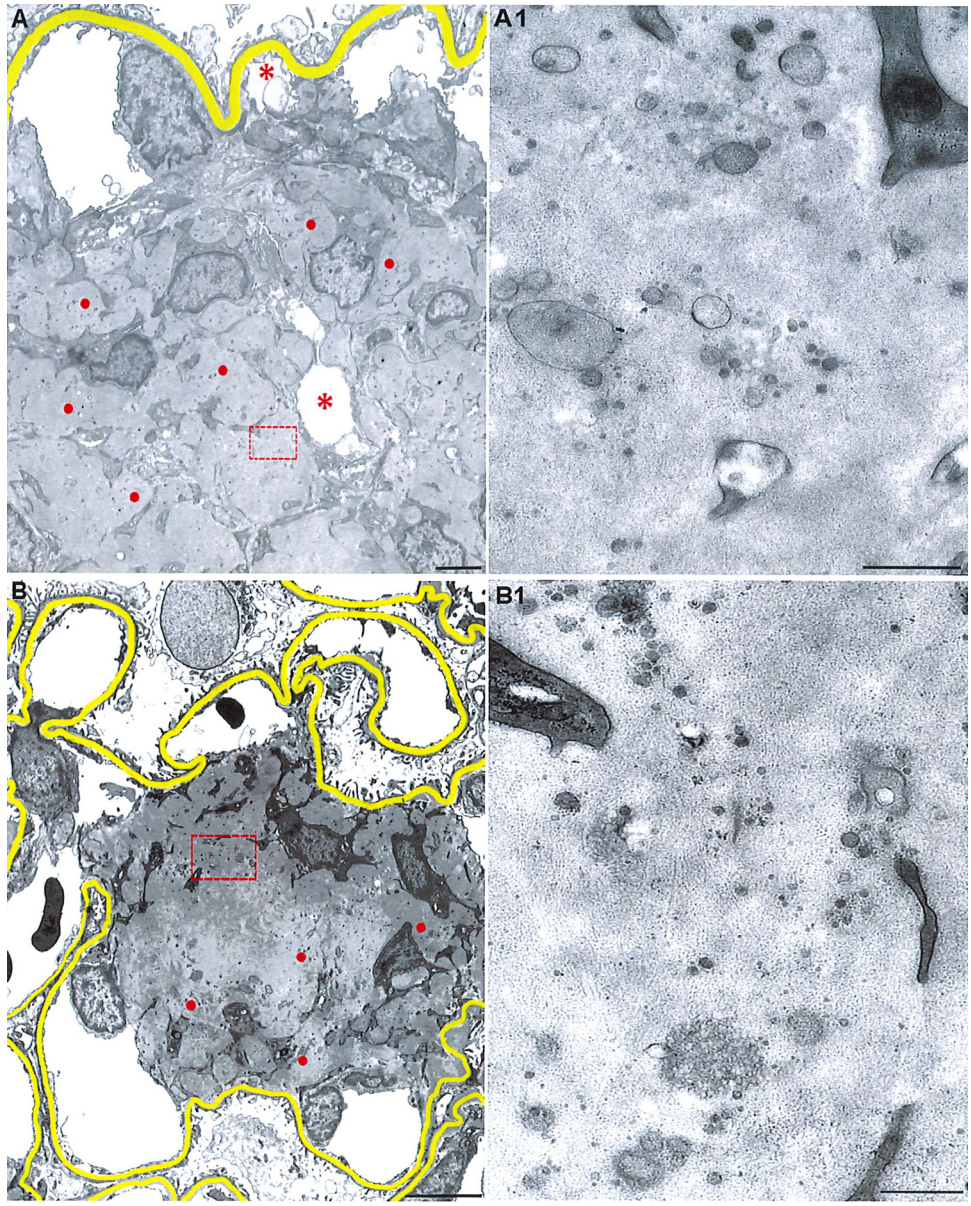

Fig. 5. Advanced stages of mesangial matrix expansion. *A/A1* transitional and *B/B1*, early stage of NS. The advanced accumulation of matrix in the mesangium can clearly be seen. Capillaries within central areas of the mesangium are in the process of disappearing (asterisks in *A*) or are fully absent (*B*). Only superficially located capillaries are left, which may exhibit normal endothelial and podocyte layers. Also mesangial cells look normal; in NS (*B*) they gather peripherally. The matrix can be identified as undegraded GBM material by its pepper-like punctuation with podocyte matrix vesicles (red dots). A delimited area with such podocyte remnants is enlarged in *A1* and *B1* clearly identifying these inclusions as various cytoplasmic structures. TEMs from DN biopsy material. Scale bars: *A*, 2.5 μm; *B*, 5.0 μm; *A1* and *B1*, 0.5 μm.

cytoplasmic portions that remained included within these portions of the GBM even after they were incorporated into the mesangium. These remnants may clearly be taken as distinctive traces in matrix portions that have recently separated from the GBM. Surprisingly, such traces may still be found in the matrix of nodules.

Our IF studies are highly supportive of this view, and they define this process more precisely. We found that in early stages of DMS the α1, α3, and α5 chains of collagen IV were accumulated within the mesangium. Their IF staining pattern, in conjunction with their staining in the GBM, suggested the direct origin of these mesangial matrix components from the GBM corresponding to the observations in TEMs. Also, the IF results concerning agrin and perlecan are supportive, showing that proteoglycans derived from the GBM also accumulate in the mesangium in DN. The strong staining for perlecan and the α1 chain of collagen IV of both the GBM and mesangial matrix in DN came as a surprise, suggesting that metabolic processes typical for the embryonic kidney have reappeared (see below).

In transitional stages from DMS to NS, the IF staining for the α3 and α5 chains of collagen IV did not accordingly increase compared with the increasing matrix accumulation seen in TEMs, suggesting either a delayed degradation or simply a loss of the antigenic domains (see below). In contrast, the IF-staining of the α1 chain of collagen IV increased in parallel with the expansion of the mesangium and was maintained even in NS. Thus, in fully developed nodules, the staining for the α3 and α5 chains of collagen IV was absent and for the α1 chain clearly present. With respect to the IF-staining of the proteoglycans in DN, the staining pattern for agrin was similar to that of α3 and α5 chains, while that of perlecan largely corresponded to the pattern of the α1 chain of collagen IV.

These findings agree with a previous study (33) in which the massive accumulation of collagen IV (no separation into

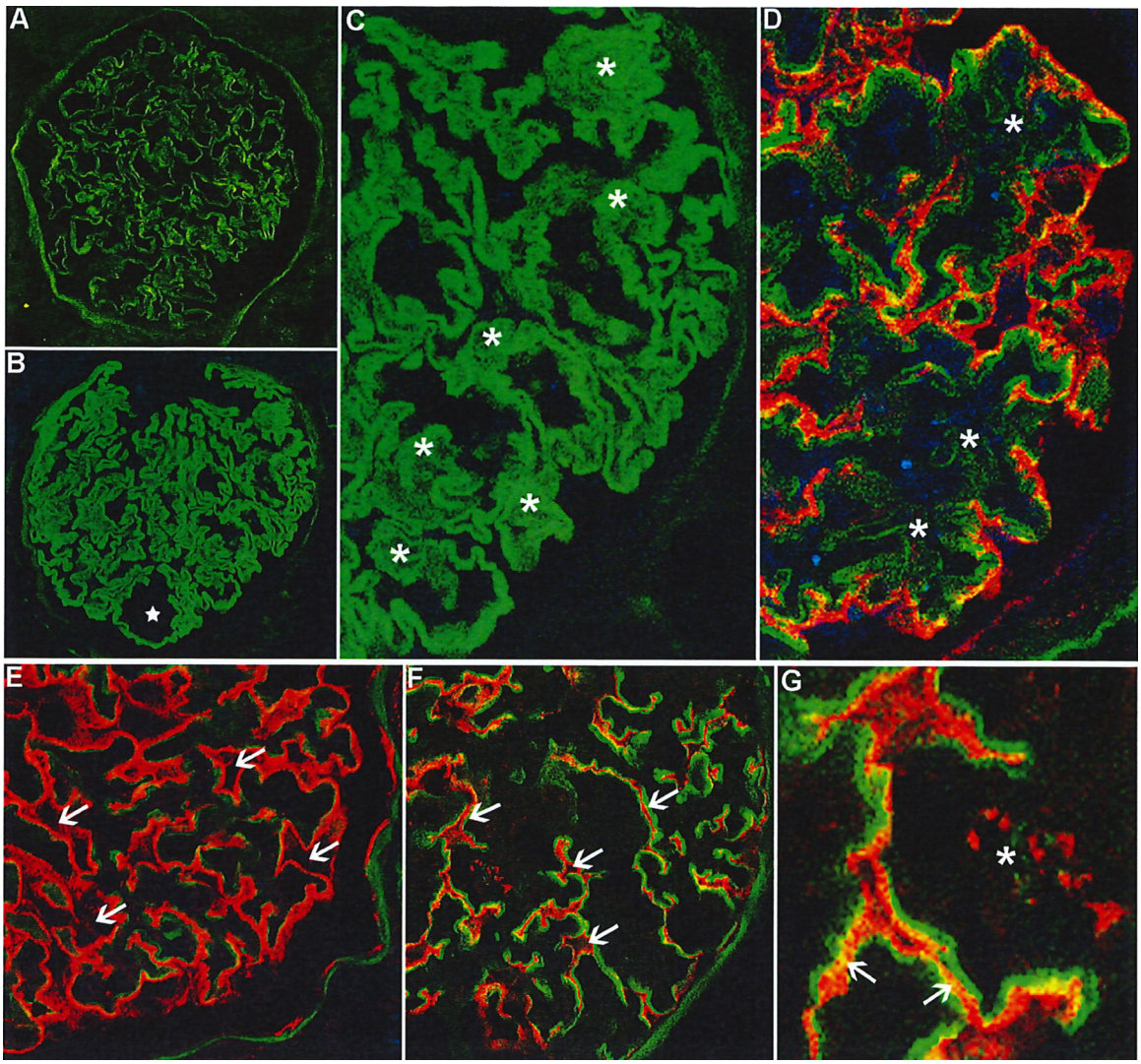

Fig. 6. Immunofluorescence (IF) data concerning the collagen IV-α5 chain. The staining pattern of the collagen IV α3 and α5 chains are almost identical; here, we show the results of the α5 chain. The GBM and deposits in the mesangium are stained. Biopsies without pathological changes served as controls. *A*: control. Note the comparably weak but continuous staining of the GBM; deposits in the mesangium are not seen. *B* and *C*: DMS. The thickened GBM is intensively stained throughout. Note the staining of deposits in the mesangium, labeled by asterisks in *C* (zoom of *B*). Central regions of the mesangium are unstained including the central core of a nodule (star in *B*). *D*: DMS, double staining with synaptopodin. In addition to the intensive staining of the GBM, deposits in the mesangium that are in continuation with the GBM are stained (asterisks). Central parts of the mesangium are not stained. *E, F*, and *G*: distinctive differences in the width of the spaces (arrows) within the GBM infoldings between control (*E*) and DMS (*F*) that are occupied by podocytes (stained red for synaptopodin). In DMS, these spaces have changed into narrow clefts, from which the podocytes seem to be squeezed out. Best seen in *G* (arrow). In addition, in *G* (zoom of *F*) incorporation of podocyte remnants into the mesangium is seen (asterisk). *A* and *E*, controls; *B, C, D, F*, and *G*, DMS. Confocal IF with an antibody against the α5 chain of collagen IV. In *D–G*, double incubation with an antibody to synaptopodin. Original magnifications, ×400.

chains) in the mesangium was shown. Kim and colleagues (24, 48) for the first time used chain-specific antibodies (albeit different from ours) and received similar results to ours concerning the α1 and α2 chains, including strong staining of the mesangium but, in contrast to our observations, a decreased but nevertheless clear staining of the peripheral GBM in DN; and with respect to α3 and α4 chains, staining of the GBM but not of the mesangium was reported.

The discrepant behavior of the α1 chain on one side and the α3 and α5 chains of collagen IV on the other may have several reasons. First, in contrast to the α3 and α5 chains the α1 chain may resist degradation. This view is supported by the observation that also in controls discrete accumulations of the α1 chain of collagen IV were encountered in the mesangium.

Second, the disappearance of the IF staining does not prove the disappearance of the material. In contrast to the α1 chain, the α3 and α5 chains of collagen IV may have lost their antigenic domains by glycation or carbonylation (12, 29, 30). Advanced glycation end products have been found in high concentrations in the mesangial matrix, specifically in DN (43). A gradual loss of the antigenicity of the α3 and α5 chains would best fit with the observations in TEMs that do not suggest any degradation.

Our ISH-studies confirm that the α3 chain of collagen IV is synthesized exclusively by podocytes and the α1 chain exclusively by endothelial cells, without a contribution by mesangial cells, here clearly shown in DN (Fig. 8*E*). Consequently, the view that the accumulated mesangial matrix in DN directly

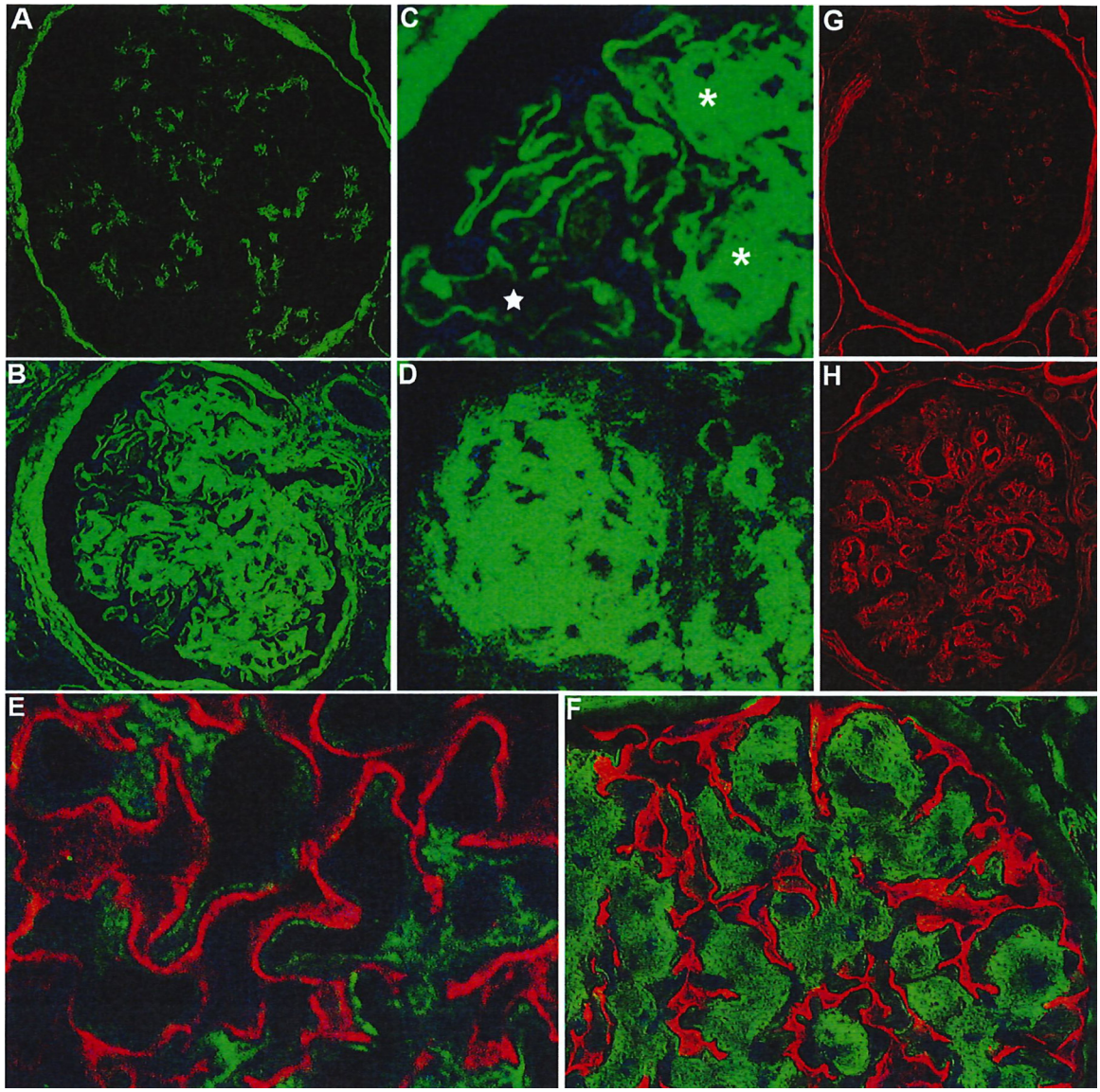

Fig. 7. IF data concerning the collagen IV-α1 chain and perlecan. The staining pattern of the α1 chain is clearly different from those of the α3 and α5 chains of collagen IV. *A* and *E*: controls displaying a weak and irregular staining of the GBM and of discrete mesangial deposits. In DMS (*B*) and (*C*, zoom of *B*), the mesangium is generally strongly stained throughout (asterisks in *C*). Staining of the GBM is heterogeneous, mostly increased, frequently very intensive even in areas that do not show much mesangial staining (star in *C*). *D*: in NS the matrix of the entire nodule is brightly stained. *E* and *F*: double incubations with synaptopodin. *E*: control; *F*: DMS. Even in controls, deposits in the mesangium are stained for the α1 chain of collagen IV; in DMS the strong mesangial staining spares only the mesangial cells. *G* and *H*: IF pattern of perlecan, control (*G*) and DN (*H*). No staining in controls; in DMS the mesangial staining is heterogeneous in its strength but comprises the entire mesangium; the staining of the GBM is at some sites very prominent. *A* and *E*: controls; *B, C, D*, and *F*: DN biopsy material. Confocal IF with an antibody against the α1 chain of collagen IV; in *E* and *F*, double incubation with an antibody to synaptopodin. *G* and *H*: IF with an antibody against perlecan; *G*, control; *H*, DMS biopsy material. Original magnifications, ×400.

derives from production within the mesangium is not supported, at least not concerning the α3 and α1 chains of collagen IV. Our semiquantitative assessments suggest that the RNA expression for the α3 chain of collagen IV in DN is equal to that in controls. Thus, there is either an overproduction of the α3 and α5 chains of collagen IV in DN triggered at the translational level, a decreased degradation of these chains, or both, that lead to the thickening of the GBM and the accumulation in the mesangium. With respect to the α1 chain of collagen IV the situation may be different. In some biopsies of DN, an increased signal number was found, suggesting that possibly an increased transcription contributed to the increased synthesis of the α1 chain (as seen in Fig. 8*F*) in DN compared with controls. This partly agrees with ISH studies in streptozotozin-induced diabetic rats, where a pronounced increase in the RNA α1 chain of collagen IV signaling was found in the total of glomerular cells (46). ISH studies in human biopsies did not reveal differences in collagen IV α1 chain RNA expression between DN patients and controls (42).

The increased synthesis of the α1 chain of collagen IV and the resumption of the production of perlecan in DN may indicate an embryonic stage of GBM synthesis (4). The change in the synthesis from the α1 and α2 chains to the α3, -4, and -5 chains of collagen IV as well as the change from perlecan to

agrin during the capillary loop stage of glomerular development is believed to be due to an increasing signaling from podocytes bringing the function of the endothelium under the dominant control of podocytes (7, 13, 34). The DN-specific thickening of the GBM may compromise the availability of paracrine signals from podocytes to endothelial cells, causing the comeback of a developmental situation. This process may regionally be different, possibly accounting for the regional heterogeneity of the immunostaining of the α1 chain of collagen IV within the GBM in DN. The dependence of the endothelial performance in the synthesis of matrix components from podocytes has been emphasized by recent coculture studies of podocytes and glomerular endothelial cells (9). In addition, and as emphasized by Abrahamson (1), various pathological conditions may interfere with the normal silencing of GBM protein gene expression, leading to renewed biosynthesis of GBM proteins.

The uncovered mechanism underlying the expansion of the mesangial matrix easily explains the fate of glomerular capillaries during the progression of DMS to NS. The shortening and finally the loss of GBM infoldings progressively deprives glomerular capillaries from contact to the GBM associated with the loss of filtration surface. Thereby, the capillaries are more and more displaced into central mesangial areas. Here, they degenerate, collapse, and finally disappear. As just discussed for the heterogeneous behavior in the synthesis of the α1 chain of collagen IV, the progressive loss of proximity to podocytes may be the culprit, in the beginning just due to the thickening of the GBM, in later stages the progressive loss of contact to the GBM, resulting in the loss of any stimulation by podocytes (7, 13, 34). Supportive of this interpretation is the observation that capillaries that maintain a superficial position opposite to fairly normal podocytes are patent and perfused and may have an endothelium with unbridged fenestrae.

Concluding Remarks

Because of these findings the turnover of the GBM takes center stage in the pathogenesis of DN. We know that under normal conditions the components of the mature GBM are synthesized by podocytes and, to a lesser degree, by endothelial cells. We do not know where under normal conditions the worn-out GBM is degraded.

A primary derailment in DN seems to be the inappropriate production of GBM material (36) including the α3 and α5 chains of collagen IV. The discussion about the stimuli for this overproduction dates back to the ’80s of the last century (40);

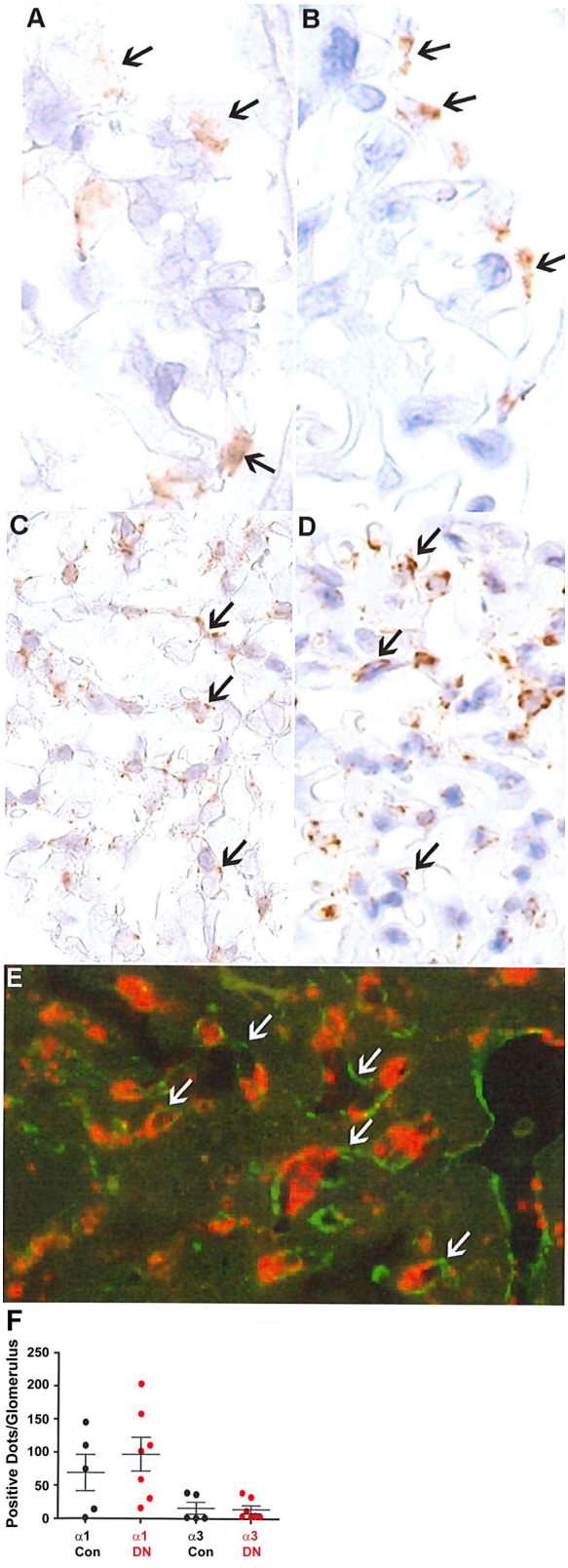

Fig. 8. In situ hybridization (ISH) for collagen IV α1 and α3 chains. *A* and *B*: ISH for collagen IV α3 chain, control and DN, showing that the mRNA signals are found in podocytes (arrows), clearly identified by their superficial localization. *C* and *D*: ISH for collagen IV α1 chain, control and DN, showing that the mRNA signals are found inside the tuft, some of which could be localized to endothelial cells (arrows); in others an assignment to either endothelial or mesangial cells was not possible. *E*: fluorescence-based ISH of collagen IV α1 chain (red) combined with IF localization of CD31 (green) clearly showing that the mRNA signals are found only in endothelial cells (arrows). *F*: quantification of the experiments shown in *A* to *D*; the results from *E* allow us to assign the signals seen in *C* and *D* to endothelial cells. Each circle represents the average number of mRNA-positive dots per glomerulus of all glomeruli in one biopsy. There is no difference in the average signal number between controls and DN with respect to the collagen IV α3 chain, whereas the heterogeneity of the signals of the collagen IV α1 chain may indicate that at least in some biopsies there is a higher signal frequency in DN. However, on average there is no significant difference. *A* and *C*: biopsy material from kidneys without pathological changes; *B*, *D*, and *E*: DN biopsy material. Original magnifications: *A*–*D*, ×400; *E*, ×200.

metabolic stimuli and/or those derived from hyperfiltration may contribute but the mediators are unknown. Recent studies in mice after inhibition of the SGLT2 decreasing hyperfiltration are conflicting (6, 17, 31, 44), but it may be deduced that the dominant influence on glomerular growth and mesangial expansion derives from blood glucose levels; assessments of the GBM-thickness after SGLT2 inhibition are not yet available. The overproduction of the α1 chain of collagen IV and the resumption of the synthesis of perlecan synthesis may be secondary effects due to the decreased availability of stimuli from podocytes by endothelial cells.

Taken together, both mechanisms, overproduction and insufficient degradation of GBM material, contribute to the progressing accumulation of matrix within the mesangium, but we do not know whether or which of both mechanisms is the main culprit. At the least, it seems from our results that the turnover, predominantly the degradation of the α1 chain of collagen IV (and suggestively also the α2 chain) and perlecan, plays a dominant role. Even if details of this process are not fully clear and need further investigation, the basic insight that worn-out GBM-material is deposited within the mesangium, accounting in large part for the mesangial matrix accumulation, is clearly shown but does not exclude that matrix components are derived from de novo production by mesangial cells, contributing to the accumulation.

This reevaluation also suggests that podocyte loss is not an early event in DN; detaching podocytes were not encountered before advanced stages of NS. This corroborates the observation that the pathological changes in DN are reversible, as it has been shown after pancreas transplantation (15) and that lesions based on podocyte loss have never been seen to be reversible.

ACKNOWLEDGMENTS

The valuable help of Brunhilde Hähnel, Hiltraud Hosser, Sylvia Kaden, Claudia Schmidt, and Rolf Nonnenmacher is greatly appreciaed.

GRANTS

We are grateful for the support of the Gotthard Schettler Gesellschaft für Herz-und Kreislaufforschung (W. Kriz), the German Red Cross Blood Service Baden-Württemberg-Hessia (W. Kriz) and the German Research Foundation, SFB1118 (H.-J. Gröne).

DISCLOSURES

No conflicts of interest, financial or otherwise, are declared by the author(s).

Parts of this manuscript had been presented at the Annual meeting of the American Society of Nephrology in San Diego 2015 (Abstract no. 3014) and in Chicago 2016 (Abstract no. 1563).

AUTHOR CONTRIBUTIONS

W.K. conceived and designed research; W.K., J.L., J.v.d.B., and H.-J.G. interpreted results of experiments; W.K. prepared figures; W.K. drafted manuscript; W.K. and H.-J.G. edited and revised manuscriptJ.L. and G.F. performed experiments; J.L., J.v.d.B., and E.G. analyzed data; W.K. approved final version of manuscript.

REFERENCES

1. **Abrahamson DR.** Role of the podocyte (and glomerular endothelium) in building the GBM. *Semin Nephrol* 32: 342–349, 2012. doi:10.1016/j.semnephrol.2012.06.005.
2. **Abrahamson DR, Caulfield JP.** Proteinuria and structural alterations in rat glomerular basement membranes induced by intravenously injected anti-laminin immunoglobulin G. *J Exp Med* 156: 128–145, 1982. doi:10.1084/jem.156.1.128.
3. **Abrahamson DR, Hudson BG, Stroganova L, Borza DB, St John PL.** Cellular origins of type IV collagen networks in developing glomeruli. *J Am Soc Nephrol* 20: 1471–1479, 2009. doi:10.1681/ASN.2008101086.
4. **Abrahamson DR, St John PL, Stroganova L, Zelenchuk A, Steenhard BM.** Laminin and type IV collagen isoform substitutions occur in temporally and spatially distinct patterns in developing kidney glomerular basement membranes. *J Histochem Cytochem* 61: 706–718, 2013. doi:10.1369/0022155413501677.
5. **Abrass CK, Peterson CV, Raugi GJ.** Phenotypic expression of collagen types in mesangial matrix of diabetic and nondiabetic rats. *Diabetes* 37: 1695–1702, 1988. doi:10.2337/diab.37.12.1695.
6. **Arakawa K, Ishihara T, Oku A, Nawano M, Ueta K, Kitamura K, Matsumoto M, Saito A.** Improved diabetic syndrome in C57BL/KsJ-db/db mice by oral administration of the Na(+)-glucose cotransporter inhibitor T-1095. *Br J Pharmacol* 132: 578–586, 2001. doi:10.1038/sj.bjp.0703829.
7. **Bartlett CS, Jeansson M, Quaggin SE.** Vascular Growth Factors and Glomerular Disease. *Annu Rev Physiol* 78: 437–461, 2016. doi:10.1146/annurev-physiol-021115-105412.
8. **Bell ET.** Renal vascular disease in diabetes mellitus. *Diabetes* 2: 376–389, 1953. doi:10.2337/diab.2.5.376.
9. **Byron A, Randles MJ, Humphries JD, Mironov A, Hamidi H, Harris S, Mathieson PW, Saleem MA, Satchell SC, Zent R, Humphries MJ, Lennon R.** Glomerular cell cross-talk influences composition and assembly of extracellular matrix. *J Am Soc Nephrol* 25: 953–966, 2014. doi:10.1681/ASN.2013070795.
10. **Camerini D Avalos RA, Caulfield JB, Rees SB, Lozano Castaneda O, Naldjian S, Marble A.** Preliminary observations on subjects with prediabetes. *Diabetes* 12: 508–518, 1963. doi:10.2337/diab.12.6.508.
11. **Chen S, Khoury CC, Ziyadeh FN.** Pathophysiology and pathogenesis of diabetic nephropathy. In: *Seldin and Giebisch's The Kidney*, edited by Alpern RJ, Caplan MJ, Moe OW. Munich: Elsevier, 2013, p. 2605–2632. doi:10.1016/B978-0-12-381462-3.00078-1.
12. **Del Prete D, Anglani F, Forino M, Ceol M, Fioretto P, Nosadini R, Baggio B, Gambaro G.** Down-regulation of glomerular matrix metalloproteinase-2 gene in human NIDDM. *Diabetologia* 40: 1449–1454, 1997. doi:10.1007/s001250050848.
13. **Eremina V, Baelde HJ, Quaggin SE.** Role of the VEGF--a signaling pathway in the glomerulus: evidence for crosstalk between components of the glomerular filtration barrier. *Nephron, Physiol* 106: 32–37, 2007. doi:10.1159/000101798.
14. **Farquhar MG: Glomerular permeability investigated by electron microscopy.** In: *Proceedings of the Conference: Small Blood Vessel Involvement in Diabetis Mellitus, Warrenton*, Virginia, 1963, edited by Siperstein MD, Colwell AR, Meyer K. Washington DC: Am Inst Biol Sci, 1964, p. 31–80.
15. **Fioretto P, Barzon I, Mauer M.** Is diabetic nephropathy reversible? *Diabetes Res Clin Pract* 104: 323–328, 2014. doi:10.1016/j.diabres.2014.01.017.
16. **Gellman DD, Pirani CL, Soothill JF, Muehrcke RC, Kark RM.** Diabetic nephropathy: a clinical and pathologic study based on renal biopsies. *Medicine (Baltimore)* 38: 321–368, 1959. doi:10.1097/00005792-195912000-00001.
17. **Gembardt F, Bartaun C, Jarzebska N, Mayoux E, Todorov VT, Hohenstein B, Hugo C.** The SGLT2 inhibitor empagliflozin ameliorates early features of diabetic nephropathy in BTBR ob/ob type 2 diabetic mice with and without hypertension. *Am J Physiol Renal Physiol* 307: F317–F325, 2014. doi:10.1152/ajprenal.00145.2014.
18. **Goldberg S, Harvey SJ, Cunningham J, Tryggvason K, Miner JH.** Glomerular filtration is normal in the absence of both agrin and perlecan-heparan sulfate from the glomerular basement membrane. *Nephrol Dial Transplant* 24: 2044–2051, 2009. doi:10.1093/ndt/gfn758.
19. **Handler M, Yurchenco PD, Iozzo RV.** Developmental expression of perlecan during murine embryogenesis. *Dev Dyn* 210: 130–145, 1997. doi:10.1002/(SICI)1097-0177(199710)210:2<130::AID-AJA6>3.0.CO;2-H.
20. **Hatch FE, Watt MF, Kramer NG, Parrish AE, Howe JS.** Diabetic glomeruloscerlosis. A long-term follow-up study based on renal biopsies. *Am J Med* 31: 216, 1961. doi:10.1016/0002-9343(61)90110-3.
21. **Hayashi H, Karasawa R, Inn H, Saitou T, Ueno M, Nishi S, Suzuki Y, Ogino S, Maruyama Y, Kouda Y, Arakawa M.** An electron microscopic study of glomeruli in Japanese patients with non-insulin dependent diabetes mellitus. *Kidney Int* 41: 749–757, 1992. doi:10.1038/ki.1992.117.
22. **Heidet L, Cai Y, Guicharnaud L, Antignac C, Gubler MC.** Glomerular expression of type IV collagen chains in normal and X-linked Alport

syndrome kidneys. *Am J Pathol* 156: 1901–1910, 2000. doi:10.1016/S0002-9440(10)65063-8.

23. **Ichinose K, Maeshima Y, Yamamoto Y, Kinomura M, Hirokoshi K, Kitayama H, Takazawa Y, Sugiyama H, Yamasaki Y, Agata N, Makino H.** 2-(8-hydroxy-6-methoxy-1-oxo-1h-2-benzopyran-3-yl) propionic acid, an inhibitor of angiogenesis, ameliorates renal alterations in obese type 2 diabetic mice. *Diabetes* 55: 1232–1242, 2006. doi:10.2337/db05-1367.
24. **Kim Y, Kleppel MM, Butkowski R, Mauer SM, Wieslander J, Michael AF.** Differential expression of basement membrane collagen chains in diabetic nephropathy. *Am J Pathol* 138: 413–420, 1991.
25. **Kimmelstiel P, Wilson C.** Intercapillary lesions in the glomeruli of the kidney. *Am J Pathol* 12: 83–98, 1936.
26. **Kriz W, Shirato I, Nagata M, LeHir M, Lemley KV.** The podocyte's response to stress: the enigma of foot process effacement. *Am J Physiol Renal Physiol* 304: F333–F347, 2013. doi:10.1152/ajprenal.00478.2012.
27. **Laipply TC, Eitzen O, Dutra FR.** Intercapillary glomerulosclerosis. *Arch Intern Med (Chic)* 74: 354–364, 1944. doi:10.1001/archinte.1944.00210230046004.
28. **Lannigan R, Blainey JD, Brewer DB.** Electron microscopy of the diffuse glomerular lesion in diabetes mellitus with special reference to early changes. *J Pathol Bacteriol* 88: 255–261, 1964. doi:10.1002/path.1700880132.
29. **Mason RM, Wahab NA.** Extracellular matrix metabolism in diabetic nephropathy. *J Am Soc Nephrol* 14: 1358–1373, 2003. doi:10.1097/01.ASN.0000065640.77499.D7.
30. **Mott JD, Khalifah RG, Nagase H, Shield CF III, Hudson JK, Hudson BG.** Nonenzymatic glycation of type IV collagen and matrix metalloproteinase susceptibility. *Kidney Int* 52: 1302–1312, 1997. doi:10.1038/ki.1997.455.
31. **Nagata T, Fukuzawa T, Takeda M, Fukazawa M, Mori T, Nihei T, Honda K, Suzuki Y, Kawabe Y.** Tofogliflozin, a novel sodium-glucose co-transporter 2 inhibitor, improves renal and pancreatic function in db/db mice. *Br J Pharmacol* 170: 519–531, 2013. doi:10.1111/bph.12269.
32. **Nasr SH, D'Agati VD.** Nodular glomerulosclerosis in the nondiabetic smoker. *J Am Soc Nephrol* 18: 2032–2036, 2007. doi:10.1681/ASN.2006121328.
33. **Nerlich A, Schleicher E.** Immunohistochemical localization of extracellular matrix components in human diabetic glomerular lesions. *Am J Pathol* 139: 889–899, 1991.
34. **Obeidat M, Obeidat M, Ballermann BJ.** Glomerular endothelium: a porous sieve and formidable barrier. *Exp Cell Res* 318: 964–972, 2012. doi:10.1016/j.yexcr.2012.02.032.
35. **Osawa G, Kimmelstiel P, Seiling V.** Thickness of glomerular basement membranes. *Am J Clin Pathol* 45: 7–20, 1966. doi:10.1093/ajcp/45.1.7.
36. **Østerby R.** Morphometric studies of the peripheral glomerular basement membrane in early juvenile diabetes. I. Development of initial basement membrane thickening. *Diabetologia* 8: 84–92, 1972. doi:10.1007/BF01235631.
37. **Østerby R.** Early phases in the development of diabetic glomerulopathy: a quantitative electron microscopic study. *Acta Med Scand Suppl* 574: 3–82, 1974.
38. **Osterby R.** Structural changes in the diabetic kidney. *Clin Endocrinol Metab* 15: 733–751, 1986. doi:10.1016/S0300-595X(86)80072-X.
39. **Price RG, Spiro RG.** Studies on the metabolism of the renal glomerular basement membrane. Turnover measurements in the rat with the use of radiolabeled amino acids. *J Biol Chem* 252: 8597–8602, 1977.
40. **Schwieger J, Fine LG.** Renal hypertrophy, growth factors, and nephropathy in diabetes mellitus. *Semin Nephrol* 10: 242–253, 1990.
41. **Suleiman H, Zhang L, Roth R, Heuser JE, Miner JH, Shaw AS, Dani A.** Nanoscale protein architecture of the kidney glomerular basement membrane. *Elife* 2: e01149, 2013.
42. **Suzuki D, Yagame M, Kim Y, Sakai H, Mauer M.** Renal in situ hybridization studies of extracellular matrix related molecules in type 1 diabetes mellitus. *Nephron* 92: 564–572, 2002. doi:10.1159/000064110.
43. **Tanji N, Markowitz GS, Fu C, Kislinger T, Taguchi A, Pischetsrieder M, Stern D, Schmidt AM, D'Agati VD.** Expression of advanced glycation end products and their cellular receptor RAGE in diabetic nephropathy and nondiabetic renal disease. *J Am Soc Nephrol* 11: 1656–1666, 2000.
44. **Vallon V, Gerasimova M, Rose MA, Masuda T, Satriano J, Mayoux E, Koepsell H, Thomson SC, Rieg T.** SGLT2 inhibitor empagliflozin reduces renal growth and albuminuria in proportion to hyperglycemia and prevents glomerular hyperfiltration in diabetic Akita mice. *Am J Physiol Renal Physiol* 306: F194–F204, 2014. doi:10.1152/ajprenal.00520.2013.
45. **Walker F.** The origin, turnover and removal of glomerular basement-membrane. *J Pathol* 110: 233–244, 1973. doi:10.1002/path.1711100306.
46. **Wu K, Setty S, Mauer SM, Killen P, Nagase H, Michael AF, Tsilibary EC.** Altered kidney matrix gene expression in early stages of experimental diabetes. *Acta Anat (Basel)* 158: 155–165, 1997. doi:10.1159/000147926.
47. **Xu X, Xiao L, Xiao P, Yang S, Chen G, Liu F, Kanwar YS, Sun L.** A glimpse of matrix metalloproteinases in diabetic nephropathy. *Curr Med Chem* 21: 3244–3260, 2014. doi:10.2174/0929867321666140716092052.
48. **Yagame M, Kim Y, Zhu D, Suzuki D, Eguchi K, Nomoto Y, Sakai H, Groppoli T, Steffes MW, Mauer SM.** Differential distribution of type IV collagen chains in patients with diabetic nephropathy in non-insulin-dependent diabetes mellitus. *Nephron* 70: 42–48, 2008. doi:10.1159/000188542.